Development of superlattice CrNNbN coatings for joint replacements deposited by High Power Impulse Magnetron Sputtering

EHIASARIAN HOVSEPIAN, Papken <http://orcid.org/0000-0002-1047-0407>, PAPKEN EHIASARIAN, Arutiun <http://orcid.org/0000-0001-6080-3946>, PURANDARE, Yashodhan <http://orcid.org/0000-0002-7544-9027>, ARUNACHALAM SUGUMARAN, Arunprabhu <http://orcid.org/0000-0002-5087-4297>, MARRIOTT, Tim and KHAN, Imran

Published version

EHIASARIAN HOVSEPIAN, Papken, PAPKEN EHIASARIAN, Arutiun, PURANDARE, Yashodhan, ARUNACHALAM SUGUMARAN, Arunprabhu, MARRIOTT, Tim and KHAN, Imran (2016). Development of superlattice CrNNbN coatings for joint replacements deposited by High Power Impulse Magnetron Sputtering. Journal of Materials Science: Materials in Medicine, 27 (9). (In Press)

Development of superlattice CrN/NbN coatings for joint replacements deposited by High Power Impulse Magnetron Sputtering

Author: 1
Prof. Papken Ehiasarian Hovsepian
Sheffield Hallam University, City Campus, Howard Street, Sheffield - S1 1WB, UK.

Author: 2
Prof. Arutiun Papken Ehiasarian
Sheffield Hallam University, City Campus, Howard Street, Sheffield - S1 1WB, UK.

Author: 3
Dr. Yashodhan Purandare
Sheffield Hallam University, City Campus, Howard Street, Sheffield - S1 1WB, UK.

Author: 4
Dr. Arunprabhu Arunachalam Sugumaran*
Sheffield Hallam University, City Campus, Howard Street, Sheffield - S1 1WB, UK.
E-mail: A.Arunachalamsugumaran@shu.ac.uk

Author: 5
Dr. Tim Marriott
Zimmer Biomet UK Limited
Dorcan Industrial Estate, Murdoch Road, Swindon - SN3 5HY, UK.

Author: 6
Dr. Imran Khan
Zimmer Biomet UK Limited
Dorcan Industrial Estate, Murdoch Road, Swindon - SN3 5HY, UK.

Abstract

The demand for reliable coating on medical implants is ever growing. In this research, enhanced performance of medical implants was achieved by a CrN/NbN coating utilising nanoscale multilayer/superlattice structure. The advantages of the novel High Power Impulse Magnetron Sputtering technology, namely its unique highly ionised plasma were exploited to deposit dense and strongly adherent coatings on Co-Cr implants. TEM analyses revealed coating superlattice structure with bi-layer thickness of 3.5 nm. CrN/NbN deposited on Co-Cr samples showed exceptionally high adhesion, critical load values of L_{C2}= 50 N in scratch adhesion tests. Nanoindentation tests showed high hardness of 34 GPa and Young's modulus of 447 GPa. Low coefficient of friction (μ) 0.49 and coating wear coefficient (K_C) = 4.94 x 10^{-16} $m^3N^{-1}m^{-1}$ were recorded in dry sliding tests. Metal ion release studies showed a reduction in Co, Cr and Mo release at physiological and elevated temperatures, (70 ^oC) to almost undetectable levels (<1 ppb). Rotating beam fatigue testing showed a significant increase in fatigue strength from 349±59 MPa (uncoated) to 539±59 MPa (coated). In vitro biological testing has been performed in order to assess the safety of the coating in biological environment, cytotoxicity, genotoxicity and sensitisation testing have been performed, all showing no adverse effects.

Keywords: Orthopaedic implant, High Power Impulse Magnetron Sputtering, Superlattice coating, Corrosion, Biocompatibility

1 Introduction

The choice of material used for medical implant components is limited by a number of factors. The material must be biocompatible, which takes into account not only the biological host response to a material but also the response of the material to the harsh mechanical and chemical environment in vivo. Human joints are bearings and as such joint replacements must be manufactured from materials that display good biocompatibility and also enhanced tribological properties in order to ensure long-term clinical performance. Due to the exacting demands the most widely used metallic materials for implant components are CoCrMo and surface treated Ti-6Al-4V alloys, however, these materials are also not without some limitations [1, 2].

One approach to enhance the performance of implants is through the deposition of a suitable biocompatible coating with better adhesion, mechanical, tribological and corrosion properties. The application of a dense ceramic layer also has the additional benefit of acting as a barrier to metal ion diffusion from the substrate, thereby reducing potential risks associated with allergic reactions. It has been reported that the corrosion resistance and biocompatibility of the CoCrMo alloy was improved with TiN films deposited by PVD technique [3]. TiN coating deposited on TiAl4V hip prosthetic head by cathodic arc evaporation exhibited a lower UHMWPE (ultra high molecular weight poly ethylene) wear rate than the uncoated head [4]. However, the failure of orthopaedic implants coated with TiN due to various factors such as in vivo fretting corrosion and third body abrasion (acrylic cement particle) has also been well documented by many authors [5]. It was reported that the deposition of DLC on CoCrMo knee component and nitrogen ion implantation (on CoCrMo or UHMWPE) improved the wear behaviour of UHMWPE compared to TiN coating on CoCrMo [6]. Serro et al. suggested that multicomponent coatings such as TiN, TiNbN and TiCN may be used for biomedical applications since no cytotoxic effect was observed for

them. Also, the wear rate of UHMWPE against TiNbN coated SS disc in the presence of albumin was low compared to TiN and TiCN coated discs [7]. Fisher et al. investigated the possibility of using TiN, CrN, CrCN and DLC coating for metal-on-metal hip prostheses [8]. Hübler et al. have reported that Ti/TiN multilayer coating deposited on 316L SS hip prosthetic femoral component exhibited better performance as compared to TiN, ZrN, Ti/TiN and Cr/V coatings [9].

Despite the multitude of coatings that have been presented, the main concern with these has been the adhesion to the substrate. In this research, enhanced performance of medical implants was attempted to be achieved by protection with a Me-Nitride based hard coating combining Nb (as one of the most chemically stable metals) and Cr (well known for its excellent tribological properties), and utilising nanoscale multilayer/ superlattice structure. Furthermore, the advantages of the novel High Power Impulse Magnetron Sputtering (HIPIMS) technology, which produces unique highly ionised plasma [10], have been exploited to deposit extremely dense and strongly adherent CrN/NbN coatings on Co-Cr implants in order to guarantee long life time when used in the demanding environment of the human body. A number of advanced surface analytical techniques and biomedical tests have been used then to characterise the properties and the performance of the new coating. Wherever possible the results have been compared with coatings deposited by more established techniques such as cathodic arc evaporation and DC magnetron sputtering.

2 Materials and Methods

2.1 Coating deposition.

CrN/NbN superlattice coatings were deposited in HTC 1000-4, four cathode system, (Hauzer Techno Coatings, Europe B.V., Venlo, The Netherlands) enabled with HIPIMS technology at Sheffield Hallam University in the United Kingdom. Prior to the coating deposition, HIPIMS

was used to pre-treat substrates to improve adhesion of the coatings. In this step the surface is subjected to intensive bombardment by Cr^+ ions generated by HIPIMS discharge on a Cr target. Due to the high ion arrival energy 1-2 keV achieved by substrate biasing, effective removal of surface oxides and other impurities takes place by sputtering (ion etching). Furthermore, a shallow (5-10 nm) implantation of Cr into the substrate material (Co-Cr, HSS, 304L SS) takes place leading to a metallurgical bonding of the coating to the substrate, which is a paramount for strong adhesion. The fundamentals and the technology for surface pre-treatment by HIPIMS metal ion etching are reported in details in [11-12]. During the coating step, HIPIMS was combined with UBM technology to benefit from the right combination of metal and gas ion rich plasma with adequate deposition rate [13]. Coating deposition was carried out in a mixed Ar + N_2 atmosphere. The coating comprises of monolithically grown CrN base layer followed by the main CrN/NbN coating utilising nanoscale multilayer/superlattice structure. CrN/NbN was deposited on prosthetic joints and 1 µm polished Co-Cr, HSS, 304L SS coupons and Si (001) wafers.

2.2 Coating characterisation

The coatings were characterised using a number of analytical techniques:

1. Coating adhesion: Coating adhesion was evaluated by scratch test. The critical load, L_{C2}, of coating-substrate system adhesive failure was measured with CSEM REVETEST equipment under progressive loading conditions, ISO 20502. Diamler-Benz test, (ISO 26443:2008) was also employed to judge adhesion quality.
2. The nano hardness and Young's modulus were measured by a CSM nanoindenter using the loading–unloading curves. MITOTOYO micro-hardness tester was used to measure the micro-hardness of specimens (load of 0.25 N).
3. Dry sliding wear coefficients (K_C), friction coefficient (µ) were determined using a pin on disk apparatus (CSM TRIBOMETER).

4. Dektak-150 stylus profiler was used to measure the depth and the profile of the wear scars as well as the roughness of the specimens.
5. Bi-layer thickness, coating texture and residual stress were determined by the glancing angle technique with the Bragg-Brentano (2θ, 20-130°) geometry in a PHILIPS XPERT XRD machine.
6. Coating microstructure was analysed using a Scanning Electron Microscopy (SEM) (FEI NOVA-NANOSEM 200). Cross-sectional Transmission Electron Microscopy (XTEM) was used for imaging and qualitative analysis of the coating-substrate interface, and the bulk of the coating by Phillips CM 430 instrument.
7. Coating corrosion resistance was evaluated by potentiodynamic polarisation tests using Gill-AC apparatus. The coated samples were polarised in a 3.5% NaCl water solution from -1000 mV to +1000 mV and the corrosion current values were recorded.
8. The fatigue strength of the coatings was determined by rotating beam fatigue testing. A range of medical tests including metal ion release, in vitro biological testing, cytotoxicity, genotoxicity and sensitisation has been performed in order to assess the safety of the coating in biological environments. A Perkin Elmer Elan 6000 inductively coupled plasma mass spectrometry (ICP-MS) was used to analyse the metal ion release.

3. Results:

3.1 CrN/NbN coating architecture, crystallographic structure and texture

Low angle X-ray diffraction (LAXRD) was used to reveal the superlattice structure of the coating. With CrN/NbN, two clear and sharp low angle reflections at $2\theta = 2.331°$ and 4.458° were observed, (XRD pattern not shown) which correspond to bi-layer thickness of $\Delta = 3.5$ nm.

Bragg-Brentano, (BB) and Glancing Angle (GA) X-ray diffractogram (XRD pattern not shown) obtained for the CrN/NbN coatings deposited on 304L SS specimens showed that the coating exhibits an F.C.C. NaCl structure with peaks appearing between the reflections of CrN or NbN with a near stoichiometric composition. A pronounced {111} texture was observed for the coating, which is in stark contrast to the DC magnetron sputtered CrN/NbN coatings, which typically develop {200} texture in standard deposition conditions. In this study, the coating thickness for both HIPIMS and DC magnetron sputtered CrN/NbN coatings was similar in the range of 4.3-5 µm.

3.2 Coating surface morphology

The surface morphology of CrN/NbN superlattice coatings deposited by cathodic arc evaporation (CA) and HIPIMS has been systematically studied by SEM and compared. The surface morphology of arc deposited CrN/NbN is shown in Fig 1a, typical for this deposition technique, macroparticle "droplet" defects are clearly visible. CA deposited CrN/NbN coating show high surface roughness values of R_a = 0.09 µm. On the other hand the surface of the HIPIMS deposited coatings appears smooth, (R_a = 0.03 µm) free of large defects. The dominating morphological feature in Fig. 1b is the hemispherical grain structure imaging the tops of the individual columns and the column boundaries of the coating.

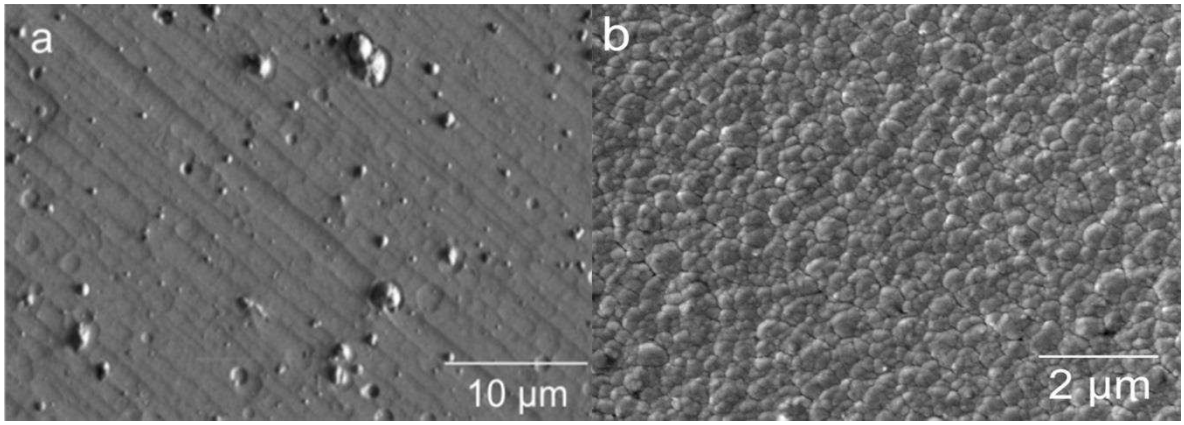

Figure 1**:** Micrographs showing the surface of the CrN-NbN coatings: a) CrN/NbN deposited by Cathodic Arc evaporation (CA) technique, b) CrN/NbN deposited by HIPIMS technique.

3.3 Coating cross section structure

The effect of the deposition method on bulk coating density was analysed by cross sectional SEM and FIB SEM analyses, Figure 2. Figure 2a is a FIB SEM image of a coating deposited by arc evaporation. A volume of the coating has been captured where a large droplet, (~ 2 µm in diameter) produced at the arc spot on the evaporation cathode has been deployed on the substrate surface at the initial stages of the coating growth. Once on the substrate, the droplet solidifies forming a pore in the centre of the feature due to the volume reduction occurring during the liquid-solid transformation. As the deposition process progresses, the coating overgrows the macro particle, (solidified droplet) which results in formation of a large dome shaped growth defect protruding a few microns above the coating surface. The growth defect engulfing the macro particle is separated from the surrounding coating by a void, which develops due to the atomic shadowing effect, but probably also due to the difference in the growth rates between the growth defect and the surrounding defect free area.

Figure 2b is a fracture cross section SEM image of HIPIMS CrN/NbN showing columnar growth. The columns are terminated with a flat surface, which correlates with the low surface roughness values, (R_a = 0.03 µm) reported above.

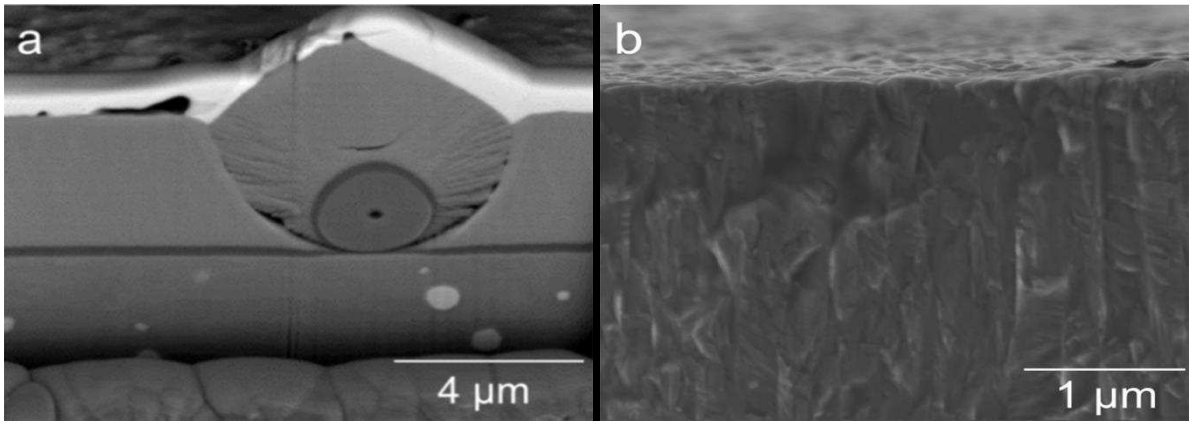

Figure 2: Cross section SEM and FIB SEM images of CrN/NbN deposited by various techniques: a) Cathodic Arc evaporation, CA, b) HIPIMS.

3.4 Structure characterisation of CrN/NbN by TEM.

Figure 3a is a lower magnification TEM image showing the coating architecturte comrising of 300 nm thick stress reducing base layer of CrN followed by the main CrN/NbN coating. The coating substrate interface appears as very sharp and free of any amorphous structured contamination or oxide layer. The higher magnification TEM image on Figure 3b reveals the superlattice structure of the coating consisting of repeating CrN and NbN layers with bi- layer thickness of Δ= 3.5 nm as calculated from the low angle XRD. The overall crystal structure is columnar, however inside of the columns a layered structure is formed due to the sequential exposure of the substrate surface to the fluxes of different materials sputtered from the targets in the coating unit during rotation.

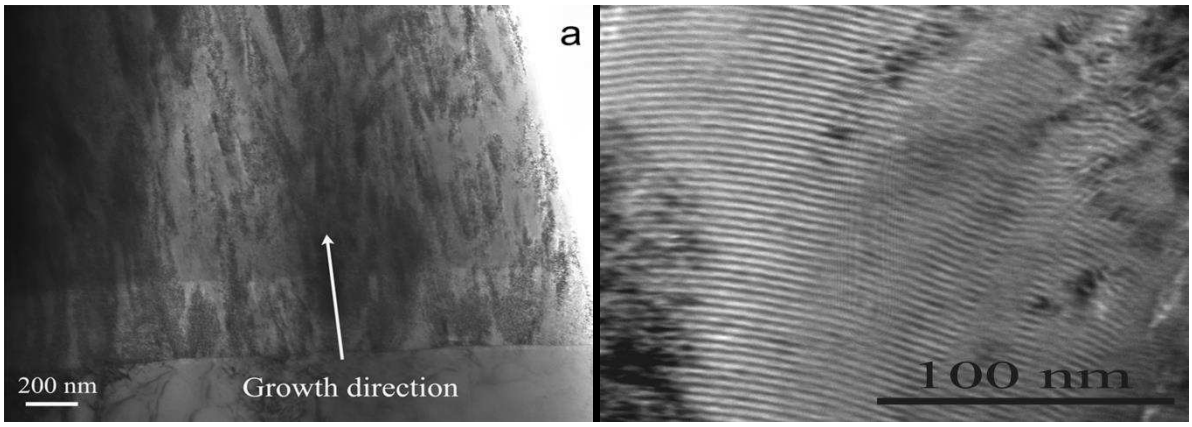

Figure 3: Bright field TEM image of CrN/NbN coatings deposited by HIPIMS at: (a) lower, and (b) higher magnifications.

The images in Figure 4 demonstrate the main differences between coating structures developed at conditions of low ad-atom mobility (deposition by DC magnetron sputtering, Figure 4a) and high ad-atom mobility (cathodic arc evaporation, Figure 4b and HIPIMS, Figure 4c). The typical structure for DC Magnetron Sputtered CrN/NbN films is columnar with high inter-columnar porosity (voids) see Figure 4a. Figure 4c is a XTEM image of CrN/NbN coating deposited by HIPIMS technology.

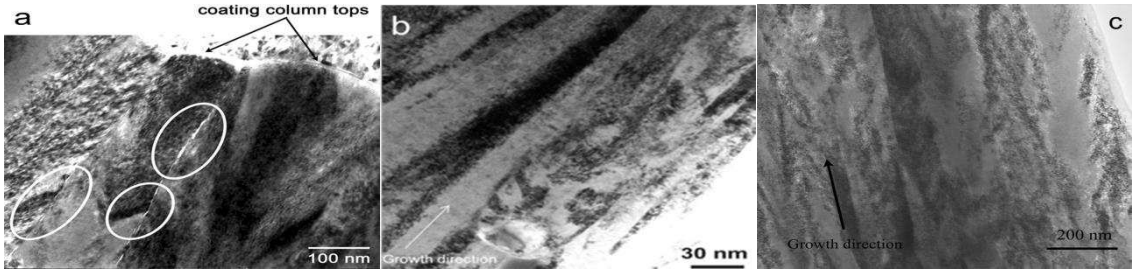

Figure 4: Bright Field -TEM images of the nanoscale CrN/NbN multilayer coating deposited by various deposition techniques: (a) DC Magnetron Sputtering, (b) Cathodic Arc evaporation, (c) HIPIMS.

3.5 CrN/NbN coating adhesion properties.

The adhesion property of CrN/NbN deposited on hardened 62 HRC high speed steel substrate was evaluated by Rockwell C indentation and scratch tests. No cracks, delamination or spallation of the coating around the Rockwell C indentation were observed thus confirming superior adhesion between the coating and the substrate. The adhesion strength in the Rockwell C indentation test can be rated as grade HF1. In addition, optical imaging of the scratch track showed no coating failure up to 100 N (L_{C2}) load.

Similarly, high adhesion was achieved on the softer Co-Cr substrate, hardness of 50 HRC. The Rockwell indent was perfect without any coating delamination around the edges of the indent or radial cracks, which classified the adhesion as grade HF1. In the scratch adhesion tests carried out on CrN/NbN deposited on Co-Cr flat coupons, no coating delamination was observed up to normal load of L_{C2}= 50 N. Compared to hardened steel, this value is lower, which is expected due to the lower load bearing capacity (lower hardness) of the substrate.

For comparison, the adhesion strength of various PVD coatings produced by different deposition techniques on femoral components of F75 CoCr, was investigated. Due to the difficulty of scratch testing upon a curved surface of a real component a novel experimental set up was developed that allowed first time a conformal trajectory of the diamond indenter

over the surface. The observed L_C values of various coatings were as follows: CA deposited ZrN/CrN: L_{C2} = 19 N, CA deposited TiNbN: L_{C2} = 38 N and HIPIMS deposited CrN/NbN: L_{C2} = 50 N, which clearly demonstrated the advantages of the novel HIPMS technology.

3.6 Mechanical and tribological properties

Both Knoop and nanoindentation gave a similar high hardness values of 3500 $HK_{0.25}$, (H_v = 3200) and Plastic hardness of 34 GPa. The Young's modulus measured in these experiments was E= 447 GPa.

Figure 5 summarises the results from wear coefficient and coefficient of friction measurements when testing uncoated and CrN/NbN coated by various techniques Co-Cr substrate in dry sliding conditions. HIPIMS deposited CrN/NbN coatings shows coefficient of friction of μ = 0.49, compared to μ = 0.9 and μ = 0.69 measured for Arc deposited coatings and bare Co-Cr substrate respectively. Correspondingly the wear coefficient of HIPIMS deposited CrN/NbN coatings of K_C = 4.9. 10^{-16} $m^3N^{-1}m^{-1}$ was found to be one order of magnitude lower than that of the arc deposited coatings and thee orders of magnitude lower that of the bare Co-Cr substrate.

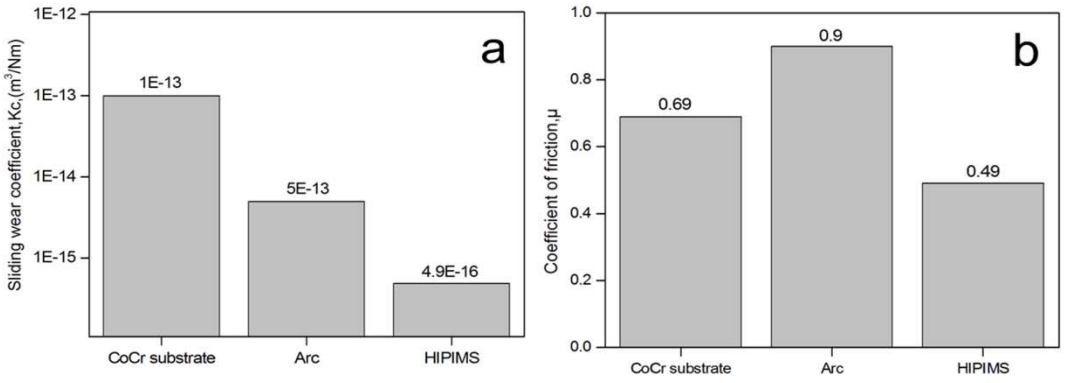

Figure 5: a) dry sliding wear coefficient (K_C) and b) friction coefficient (μ) for CrN/NbN multilayer coating deposited by various techniques on Co-Cr substrate.

3.7 Corrosion performance

Potentiodynamic polarisation method was used to understand the corrosion properties of various PVD coatings and the uncoated Co-Cr substrate material. As observed, uncoated

Co-Cr had the lowest E_{Corr} potential (-533 mV) of all the specimens tested suggesting the lowest corrosion resistance against the medium used. CrN/NbN coated specimens exhibited highest E_{Corr} potential (-284 mV) followed by TiN/NbN (-365 mV) and TiCN/NbCN (-390 mV). At anodic potentials (up to 600 mV) CrN/NbN coated specimens recorded the lowest corrosion currents, whereas for potentials more than 600 mV only TiN/NbN coated specimens exhibited lower corrosion currents.

3.8 Coating effect upon the mechanical performance of medical alloys

Mechanical characterisation of coated components has been performed in order to assess the effect of the coating upon the substrate materials. Rotating beam fatigue testing in accordance with ASTM F1160 (2014) was performed upon coated and uncoated ASTM F75 alloy, showing a significant increase (T test $P<0.001$) in fatigue strength from 349±59 MPa (uncoated) to 539±59 MPa (coated).

3.9 Performance of CrN/NbN coated implants in biological test conditions.

The metal ion release of the substrate into solution has been examined. ASTM F75 alloy bars representative of finished orthopaedic products were manufactured, cleaned and sterilised in a manner representative of packaged orthopaedic devices. Two sets of coated (n=3) and uncoated samples (n=3) were submerged in 400g of ultrapure water and compared to control and spiked samples. These were then incubated at 37 and 70°C for 28 days, representing physiological and accelerated (more severe) conditions. After initial immersion, a sample of water was taken as the 0h time point and then after 1, 7, 14 and 28 days a sample (10g) of liquid was taken and stored for analysis. The analysis was performed with a Perkin Elmer ELAN 6000 ICP-MS. The metal ion release showed a reduction in Co release at physiological and elevated temperatures over a 28 day period to undetectable levels (<1 ppb) as compared to a peak of 5 ppb for uncoated samples. The release of Cr and Mo from the substrate and coated material was below the level of detection. The results from ion release

tests for Cr, Co and Mo at different time periods taken at low (37°C) and high (70°C) temperatures are shown in Figure 6 (a-f).

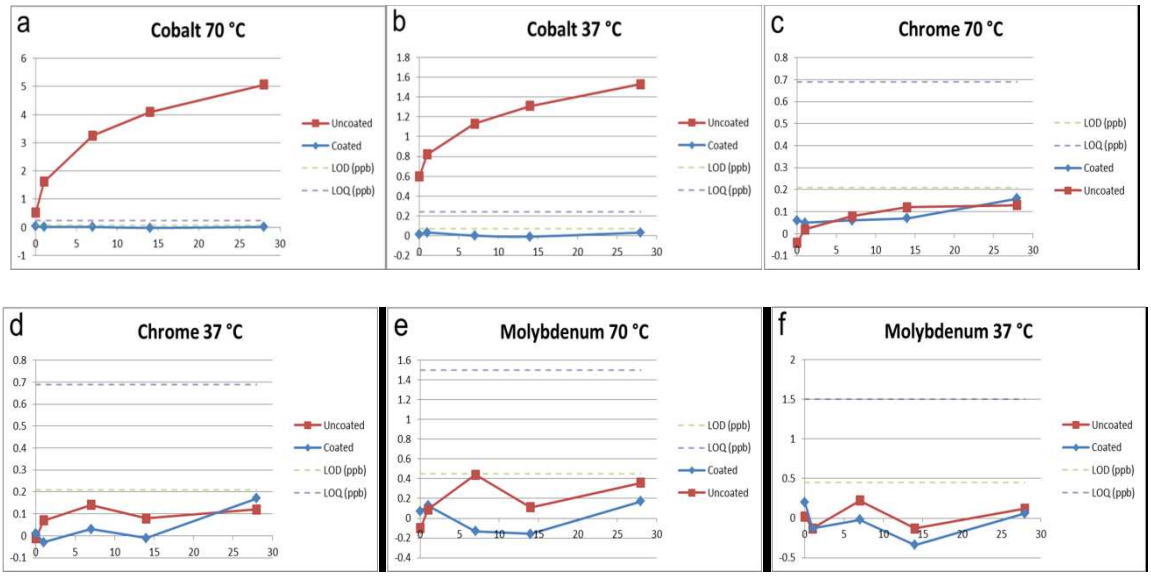

Figure 6: Ion release tests for Cr, Co and Mo at different time periods taken at high (70°C) and low (37°C) temperatures. LoD – Limit of detection, LoQ – Limit of quantification.

Not only is it important to assess the chemical and physical properties of the coating and coated substrates for orthopaedic applications, it is essential that the biological interaction with the coating is assessed. In vitro biological testing has been performed in line with the requirements of ISO 10993 in order to assess the safety of the coating in biological environments, cytotoxicity, genotoxicity and sensitisation testing have been performed, all showing no adverse effects.

4. Discussion

4.1 CrN/NbN coating architecture, crystallographic structure and texture: The highly energetic deposition flux generated by the HIPIMS discharge, (average energies typically in the range of 2-3 eV compared to energies less than 1 eV in standard DC sputtering [10,14]) provides for high ad-atom mobility during coating growth which in turn suppresses interface-roughening effects. Bombardment of the growth surface with higher energy species is an efficient tool for re-sputtering of loosely bonded atoms, which further reduces the interface

roughening. Due to the enhanced mobility of the condensing species in HIPIMS [10], sharp interfaces in CrN/NbN superlattice structured coatings can be produced at much lower bias voltage. This is reflected by the presence of sharp low angle reflections in the LAXRD pattern which in turn demonstrates the high precision of the nanolayered structure of the coating. Furthermore, it has been shown that with the use of HIPIMS technology, effective texture manipulation can be achieved by varying the peak power density applied to the sputtered target material, which in turn defines the energy of the ionised material flux emitted from the sputtered surface [14]. In the current work a pronounced {111} texture was recorded by GAXRD. It needs to be pointed out that in PVD coatings the {111} texture provides for higher wear resistance and therefore is more desirable for wear application.

Coating surface morphology and cross section structure: Figure 1 demonstrates the tremendous effect of the deposition technique on the surface structure. Despite the high melting point of Nb and the high vapour pressure and high sublimation rate of Cr the surface of the coatings produced by arc evaporation is densely covered with the globular shape macro-particle defects ranging from nanometers to microns in size. These are generated by the molten phase, (droplets) emitted from the arc spots on the cathode surface during coating deposition. This phenomenon is well understood and widely published in the literature since the invention of the process. CA deposited CrN/NbN coating show high surface roughness therefore often further mechanical polishing is needed to achieve the required surface finish for medical applications. In stark contrast, the coatings deposited by HIPIMS technology produces smooth, free of large growth defects coatings. The HIPIMS technology benefits from the utilisation of droplet free plasma and the availability of highly mobile condensing species produced in this highly ionised discharge.

Similarly, the deposition technique influences the overall density of the coating. Although the bulk of the CA deposited coatings coating is highly dense the void around the macroparticle

defect as shown in Fig. 2a directly connects the coating surface with the substrate, which largely compromises the barrier properties of the coating against environmental attack. In comparison coatings deposited by the highly ionised macroparticle free HIPIMS plasma show high overall coating density and therefore provide better protection of the substrate. Detailed analyses by TEM of the coating substrate interface region revealed the effect of the metal ion etching using metal ions produced by the HIPIMS discharge on the coating growth. The atomically clean surface of the substrate which can be achieved with such a surface pre-treatment provides conditions for local epitaxial growth. As previously shown for the CrAlN/CrN in these conditions, the local epitaxial growth can be observed on large areas (in order of several μ^2) on the surface. Coating orientation determined by some of the substrate grains can be retained from the interface to the top of the coating [15] . This peculiar coating growth mechanism strongly improves coating density and adhesion. The high coating density in HIPIMS results from the high ad-atom mobility due to the high energy of the arriving condensing species. In such conditions the ad-atoms have enough energy to bridge the gaps between the individual columns and produce very dense structure, which is superior to the coating structure formed by standard low energy DC magnetron sputtering, see Fig 4 a and c.

Adhesion Property: An excellent adhesion of PVD coatings to the substrate is of paramount importance in all applications. It has been shown that the life time of milling tools in dry cutting operations for example is proportional to the critical load measured in scratch adhesion testing [16]. However, in the case of medical implants special care has to be taken to ensure high adhesion, as coatings adhesion failure not only has implications on the coating wear life-time, but could lead to premature failure of the implant and severe health implications for the patients. Conventional methods utilise Ar glow etching or Cathodic Arc discharge pre-treatments that have the disadvantage of producing weak (amorphised)

interfaces in the former case or adding droplets at the interface in the latter case. Due to the plasma characteristics, HIPIMS provides a powerful tool for interface engineering, avoiding macro-particle defects and retaining the crystallinity of the interface [12].

Plasma diagnostic studies Cr HIPIMS discharge used for surface pre-treatment of the substrate prior to the CrN/NbN coating showed that the plasma is dominated by Cr^{1+} ions with a relative content of 60.5%. A significant observation is the presence of Cr^{2+} and Cr^{3+} ions, making a combined relative percentage of 15%, along with Ar^{1+} ions (23%), Ar^{2+} ions (2%) [17]. Thus it revealed that HIPIMS has a high content of metallic ions resulting in a metal ion-to-gas ion ratio of approximately 3:1. During the pre-treatment step a peak substrate current density (Js) of 155 mA cm^{-2} was recorded. In comparison the substrate current density in conventional sputtering and arc discharges is in the range of 5 mA cm^{-2}. This indicates that during HIPIMS pre-treatment, the substrate surface is bombarded with a high intensity ion flux which, as shown by the mass spectroscopy analysis, contains mainly metal ions. Transmission electron microscopy, (Figure 7) has shown that Cr is implanted to a depth of 10-50 nm into the substrate surface, modifying the structure in such a way that localised epitaxial growth of the condensing film occurred. The HIPIMS pre-treatment promoted a strong alignment of the orientation of the coating structure with polycrystalline substrate grains. This is due to the combination of incorporated metal ions and the preservation of crystallinity of the substrate. Evidence and conditions for the formation of cube-on-cube epitaxy on steel is shown in Figure 7. Figure 7 reveals the substrate/base layer interface after HIPIMS pre-treatment. A clearly defined transition between substrate and CrN base layer is observed. The base layer grows in a dense columnar microstructure, which can be attributed to the high energy of particles in the arriving ion flux and therefore high ad-atom mobility of the condensing species. The image includes a selected area (diameter 160 nm) diffraction pattern of the interface region. It can be observed that the diffraction spots

appear as doublets, which represents the two crystals of the substrate and the base layer. The two crystals exhibit a similar orientation with a slightly different lattice parameter. It can be seen that the two crystals are highly aligned with each other giving a clear indication of a hetero-epitaxial growth of the coating on the substrate, which is a paramount condition for high coating adhesion. The surface pre-treatment using HIPIMS is a patented technology [11] where the fundamentals of the process are described by Ehiasarian et al [12].

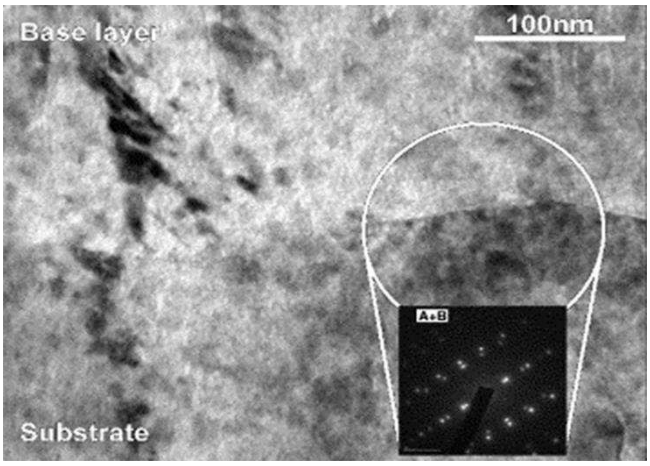

Figure 7: HIPIMS pre-treated substrate/base layer interface and selected area diffraction pattern with diffraction spots from substrate and base layer [18].

This paper reports first time a significantly enhanced adhesion, Lc=50N of hard coating such as CrN/NbN deposited on Co-Cr alloys used for the manufacturing of medical implants. The critical load in scratch adhesion test value Lc in the HIPIMS case is almost double as higher when compared to these achieved by Cathodic Arc deposition, (Lc= 19N for ZrN/CrN and Lc= 38N for TiNbN). It is important to point out that both HIPIMS and CA technologies use similar surface pre-treatment approach when metal ions are implanted into the substrate material. However, in the case of the CA technology a significant portion of the substrate surface area, (up to 19% for Cr etching and 27% for Ti etching) gets covered by droplets during the pre-treatment stage. These droplets are not strongly bonded to the surface and therefore reduce the true surface area contributing to the adhesion strength. This research confirms also the importance not only of securing a strong metallurgical bonding between the

substrate material and the coating, which is achieved by metal ion implantation but also the importance of utilising droplet free plasma for the pre-treatment.

4.2 Mechanical and tribological properties: The high plastic hardness of 34 GPA measured by nanoindentation puts the CrN/NbN coating close to the class of the super-hard materials, with plastic hardness higher than 40 GPa [19]. This high hardness of the coating can be attributed to the nanoscale multilayer structure as well as to the utilisation of HIPIMS during coating growth.

It is well understood that the hardness of the material defines its tribological properties and most particularly its wear resistance. In the case of medical articulating implants, the wear mechanism is complicated and based on a combination of abrasion, adhesion, fatigue and corrosive processes. These processes result in the generation of wear debris of which the geometric size and chemistry influence the biological interaction with these particles. One of the advantages of the nanoscale multilayer superlattice structured coatings (besides the enhanced hardness values) is their special wear mechanism due to the role of the interfaces between the individual layers. For multilayers in general, the interfaces have been postulated as sites for elastic energy dissipation and crack deflection [20]. The columnar structure monolithically grown single layer coatings however, show very different wear behaviour. The individual columns of the monolithically grown coatings experience severe plastic deformation, which leads initially to bending in the direction of sliding and finally to their mechanical breakage. The observed depth of these failures, defines the size of the wear debris generated in the tribo- contact, which reaches typically 50 to 75 nm. In contrast for coatings exhibiting superlattice structure the predominant wear mechanism is layer by layer wear with a typical wear depth of 6 to 8 nm only, which releases extremely fine wear particles [16]. This mechanism also defines the coefficient of friction as well as the wear resistance of the tribological couple.

As expected the high hardness of the coating has resulted in 2-3 orders of magnitude increase of the wear resistance compared to the bare substrate. Owing to its high density and excellent adhesion in this test, HIPIMS deposited CrN/NbN coating outperformed the arc coatings.

To understand the reasons behind the superior tribological performance of the CrN/NbN, Raman analysis was extensively used to reveal the phase composition of the tribo-film and the wear debris produced during dry sliding against Al_2O_3 in ambient atmosphere. The spectra taken in the wear track is shown in Figure 8. Three different compounds (oxides) were identified namely, Cr_2O_3, Nb_2O_5 and mixed $CrNbO_2$ in addition to the CrN/NbN coating. This confirms that the predominating wear mechanism in dry sliding test conditions is oxidative wear, where the coating elements react with the oxygen from the atmosphere due to the high flash temperatures at the asperity contacts. The low friction coefficient of CrN/NbN can be attributed to the crystal structure of the Cr_2O_3. The crystal structure of the eskolaite is based on a hexagonal close-packed (hcp) lattice, where each metal site is surrounded by an oxygen octahedron. Structures based on a regular three dimensional network of oxygen octahedra partially filled with metal atoms are typical called Magnély phases [21] known for V, Ti, Nb and W. The in situ formation of Magnély phases in the wear track and their performance as a highly lubricious tribofilm reducing friction and wear has been widely reported [22]. Mechanical characterisation of these oxides has shown that they have the capacity of elasto-plastic deformation so that high shear stress and normal pressure can be supported by this tribo-film without increase of frictional stress. Owing to its structure Cr_2O_3 shows similar behaviour in the tribological system, effectively reducing friction and wear. This behaviour can be attributed to the arrangement of Cr atoms in the (h.c.p.) lattice, which has a limited ductility due to the small number of slip systems operating under applied external load and therefore reduced capacity for elasto-plastic deformation. It is a general rule

in tribology that the friction coefficient, μ, is directly related to the ductility of the material, as the ductility of the metal increases so does the value of μ [23]. It should be expected that when implanted in the human body the tribological behaviour of the coating will show similar behaviour of tribo-film formation due to the mechanical load as well as formation of various compounds due to tribo-chemical reactions with the body fluids.

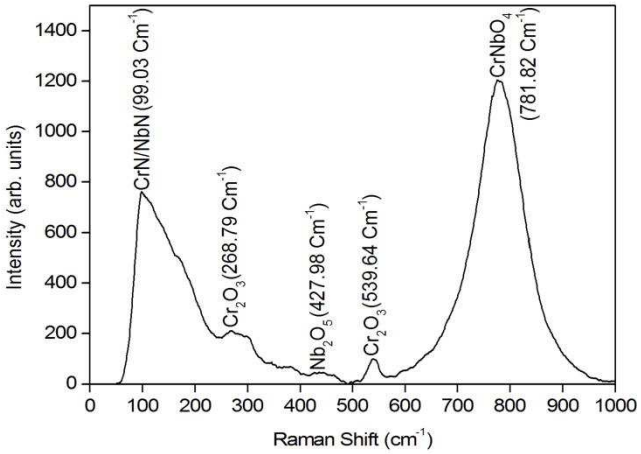

Figure 8: Raman spectra taken in the wear track of CrN/NbN sliding against Al_2O_3 counterpart.

4.3 Coating effect upon the corrosion and mechanical performance of medical alloys: The corrosion resistance of a coating is dependent on its inherent chemical inertness along with factors such as its structural density, integrity and defect density. The experiments suggest that compared to TiCN/NbCN and TiN/NbN, the CrN/NbN coated specimens were the most corrosion resistant owing to their elemental constitution, coating architecture and high density. Nb as one of the coating elements is known for its electrochemical stability. In corrosion conditions, Nb passivates forming extremely dense Nb_2O_5 film, which hinders the corrosion attack. The extremely large number of interfaces between the individual CrN and NbN layers in the superlattice coating, (over 2000 for 4μm thick coating with bi-layer thickness of Δ= 3.5 nm) provide effective barrier against coating penetration by the corrosive media. Similarly the high coating density as shown in Figs 3a, and Fig.4c improve tremendously the protective properties against environmental attack.

The deposition process, coating defects and additional roughness generated by coatings are generally considered as a reason for reduction of the fatigue strength of the underlying substrate [24]. This phenomenon is well studied for critical high-tech engineering applications such as aero-engine turbine blades, where often due the fatigue deficit experienced by the base material, the application of coatings has been avoided all together. This certainly is one of the big challenges for the coating and deposition method selection process for medical articulating implants. However, the positive result showing a significant increase (T test $P<0.001$) in fatigue strength from 349±59 MPa (uncoated) to 539±59 MPa (coated) achieved first time by a PVD process is very encouraging.

It is believed that the fatigue strength increase after coating deposition by HIPIMS can be attributed to two effects. The first effect is the increased compressive stress levels in the substrate surface due to the metal ion implantation during the pre-treatment stage. It is well known that the presence of compressive stress at the surface of the material hinders tensile crack formation and propagation. Secondly the low surface roughness and low surface defect density achieved by HIPIMS reduces the number of the potential sites for crack initiation. The combination of these two features of the HIPIMS coatings is thought to result in the significantly increased fatigue life of the substrate. As fatigue properties are known to be largely geometry and surface finish dependant orthopaedic components manufactured from ASTM F75 alloy were tested to physiologically relevant load levels. The coated implants exceeded the expected load requirements and those stipulated in ASTM F1800 showing the suitability of the CrN/NbN coating for use in orthopaedic load bearing applications.

4.4 Performance of CrN/NbN coated implants in biological test conditions: The significant reduction of Co ion release shown in long term (over a 28 day period) physiological and elevated temperatures tests to undetectable levels (<1 ppb, Fig. 6 a,b) as compared to a peak of 5 ppb for uncoated samples can be attributed to the excellent barrier properties of the

CrN/NbN. The negligible, below the level of detection release of Cr and Mo from the substrate and coated material, Fig.6 (c-f) result from the high electrochemical stability of the coating materials as well as the high coating density and extremely low level of coating growth defects achieved thanks to the utilisation of the HIPIMS technology. These enhanced coating properties are also the primary reason for the reliable performance of the CrN/NbN coating (no adverse effects) in biological environments, cytotoxicity, genotoxicity and sensitisation tests carried out In vitro.

5. Conclusions:

The synergy between smart material combination, unique coating structure and advanced deposition method has been successfully exploited to produce a novel high quality application tailored CrN/NbN coating which is a promising candidate representing the next generation of coatings for medical implants. The mechanical properties of the coating are far superior to that of conventional PVD coatings offering improved adhesion and wear performance. The biological performance and improvement in corrosion resistance, and as a result metal ion release, makes this a promising solution for patients with metal ion sensitivity. Another important finding with this coating is the improvement in fatigue strength that it imparts on the substrate. This improvement in fatigue life may provide an additional benefit by allowing the development of thinner sectioned more bone-conserving designs of orthopaedic components.

6. References:

1. Biomet knee Joint Replacement Prostheses. In: Knee joint replacement. Metro Biosol Pvt. Ltd. 2010. http://www.biosol.co.in/pdf/01-50-0975.pdf.
2. Okazaki Y, Gotoh E. Comparison of metal release from various metallic biomaterials in vitro. Biomaterials. 2005; 26(1):11-21.
3. Pham VH, Yook SW, Lee E J, Li Y, Jeon G, Lee JJ, Kim HE, Koh YH. Deposition of TiN films on Co–Cr for improving mechanical properties and biocompatibility using reactive DC sputtering. J. Mater. Sci. Mater. Med. 2011; 22(10): 2231-7.
4. Coll BF, Jacquot P. Surface modification of medical implants and surgical devices using TiN layers. Surf. Coat. Tech. 1988; 36(3–4): 867-78.
5. Raimondi MT, Pietrabissa R. The in-vivo wear performance of prosthetic femoral heads with titanium nitride coating. Biomaterials. 2000; 21(9): 907-13.
6. Oñate JI, Comin M, Garcia A, Vivente JL, Brizuela M, Garagorri N, Peris JL, Alava JI. Surf. Coat. Tech. 2001;142-144:1056-62.
7. Serro AP, Completo C, Colaço R, dos Santos F, Lobato da Silva C, Cabral JMS, Araújo H, Pires E, Saramago B, Surf. Coat. Tech. 2009; 203(24):3701-7.
8. Fisher J, Hu XQ, Stewart TD, Williams S, Tipper JL, Ingham E, Stone MH, Davies C, Hatto P, Bolton J, Riley M, Hardaker C, Isaac GH, Berry G. Wear of surface engineered metal-on-metal hip prostheses. J. Mater. Sci. Mater. Med. 2004;15:225-35.
9. Hübler R, Cozza A, Marcondes TL, Souza RB, Fiori FF. Wear and corrosion protection of 316-L femoral implants by deposition of thin films. Surf. Coat. Tech. 2001; 142-144:1078-83.
10. Ehiasarian AP. Fundamentals and applications of HIPIMS. In: Wei R, editor. Plasma Surface Engineering Research and its Practical Applications, Trivandrum: academic; 2008.pp.35-85.

11. Ehiasarian AP, Hovsepian PEh, Münz W-D, Patent: EP 1 260 603 A2, DE 10124749, 21.05. 2001.
12. Ehiasarian AP, Wen JG, Petrov I. Interface microstructure engineering by high power impulse magnetron sputtering for the enhancement of adhesion. J. Appl. Phys. 2007; 101:05430- 40.
13. Hovsepian PEh, Sugumaran AA, Purandare Y, Loch DAL, Ehiasarian AP. Effect of the degree of high power impulse magnetron sputtering utilisation on the structure and properties of TiN films. Thin Solid Films.2014; 562, 132-9.
14. Ehiasarian AP, Vetushka A, Aranda Gonzalvo Y, Sáfrán G, Székely L, Barna PB, Journal of applied physics, Influence of high power impulse magnetron sputtering plasma ionization on the microstructure of TiN thin films. 2011; 109:104314 - 29.
15. Sáfrán G, Reinhard C, Ehiasarian AP, Barna PB, Székely L, Geszti O, Hovsepian PEh. Influence of the bias voltage on the structure and mechanical performance of nanoscale multilayer CrAlYN/CrN physical vapor deposition coatings. J. Vac. Sci. Technol. A.2009; 27:174.
16. Hovsepian PEh, Münz W-D. Synthesis, Structure, and Applications of Nanoscale Multilayer/Superlattice Structured PVD Coatings. In: Cavaleiro A, De Hosson JThM, editors. Nanostructured Coatings, New York: academic; 2005.pp.555-644.
17. Hovsepian PEh, Ehiasarian AP, Purandare YP, Braun R, Ross IM. Effect of high ion irradiation on the structure, properties and high temperature tribology of nanoscale CrAlYN/CrN multilayer coating deposited by HIPIMS-HIPIMS technique. Plasma Processes Polym.2009; 6(1):S118–23.
18. Reinhard C, Ehiasarian AP, Hovsepian PEh. CrN/NbN superlattice structured coatings with enhanced corrosion resistance achieved by high power impulse magnetron sputtering interface pre-treatment. Thin Solid Films. 2007; 515:3685-92.

19. Chu X, Barnett SA, Wong MS, Sproul WD. Reactive unbalanced magnetron sputter deposition of polycrystalline TiN/NbN superlattice coatings. Surf. Coat. Technol. 1993; 57:13-18.
20. Holleck H, Schier V. Multilayer PVD coatings for wear protection. Surf. Coat. Technol. 1995; 76-77: 328-36.
21. Skopp A, Woydt M. Ceramic and Ceramic Composite Materials with Improved Friction and Wear Properties. Trib. Trans. 1995; 38(2): 233-42.
22. Woydt M, Skopp A, Doerfel I, Witke K. Wear engineering oxides/anti-wear oxides. Wear. 1998; 218: 84-95.
23. I.M. Hutchings. Tribology: Friction and Wear of Engineering Materials.1st ed. Oxford: Elsevier science & Technology; 1992.
24. Costa MYP, Venditti MLR, Cioffi MOH, Voorwald HJC, Guimarães VA, Ruas R. Fatigue behavior of PVD coated Ti–6Al–4V alloy. Int. J. Fatigue. 2011; 33(6):759-65.